A Curvature based Method to Extract Natural Landmarks for Mobile Robot Navigation

Pedro Núñez, Ricardo Vázquez, José C. del Toro, Antonio Bandera and Francisco Sandoval
Grupo de Ingeniería de Sistemas IntegradoS, Dpto. Tecnologia Electronica, E.T.S.I. Telecomunicacion
Universidad de Malaga, Campus de Teatinos 29071-Malaga (Spain)
Email: pmnt@uma.es

Abstract **– Landmark extraction is an essential task for robot navigation which not only requires an effective measure, but also the characterisation of landmarks to reduce the subsequent data association ambiguity. This paper describes a new method to detect natural landmarks from the adaptively estimated curvature function associated to 2D laser scans. This set of landmarks is composed of items associated to real and virtual features of the environment (corners, center of tree-like objects, line segments and edges). A novelty of the proposed system is that, for each landmark, characterisation provides not only the parameter vector, but also complete statistical information. Experimental results show the effectiveness of this method to deal with structured environments.**

Keywords **– Natural landmark extraction, Mobile robot navigation, Adaptive curvature estimation**

I. Introduction

The success of the most of the tasks that facilitates robot navigation as simultaneous localisation and map building (SLAM), are conditioned by an accurate estimation of the robot pose to obtain a good map and an effective data association process. In order to increase the efficiency and robustness of this process, it is helpful that sensor data is transformed in a more compact form before attempting to compare them to the ones presented on a map or store them in the map that is being built. The chosen map representation heavily determines the precision and reliability of the whole task. In our case, we have chosen a landmarkbased approach for map representation. The main advantages of this kind of approach is to allow the use of different models to describe the measurement process for different features of the environment and to avoid the data smearing effect [9]. However, the success of a landmark-based representation is highly conditioned on the chosen type of landmark and on the availability of fast and reliable algorithms capable of extracting landmarks from a large set of noisy and uncertain data. Typically, structured environments have common geometry features which can be described by polygonal items in a planar map representation. Corners [1, 6], line segments [3, 11] or tree-like objects [12] have been used to represent only geometrical information of the environment. The aim of this work is to extract and characterise simultaneously several types of landmarks that are present in structured environments using a 2D laser range scanner (see Fig. 1). The approach must be fast and capable of extracting landmarks from noisy uncertain data. Moreover, the system must provide not only geometrical landmark description, but also statistical information to use in later task for navigation, as SLAM. In a previous version of this work [8], the adaptive curvature function was directly used to provide corners, line and curve segments. However, parameter vectors extracted from this curvature function are noisy and the algorithm does not provide information about the uncertainty matrices associated to the landmarks. The proposed system uses this curvature function to segment the laser scan into sets of range readings which present a similar curvature value.

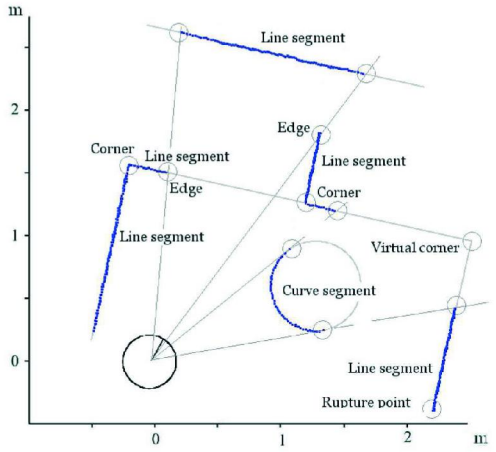

Fig. 1. Set of natural landmarks obtained from a 2D laser scan.

This paper is organized as follows: Section 2 and 3 briefly describe the characteristics of the data pre-processing and the laser scan data segmentation algorithms, respectively. Detection

and characterisation of the different landmarks (real and virtual corners, edges, and line and curve segments) is shown in Section 4. Section 5 presents experimental results and, finally, Section 6 summarizes conclusions and future work.

II. Laser Scan Data Acquisition and Pre-processing

Range images provided by laser sensors are typically in polar coordinates, $\{(r,\phi)_l | l = 1...N_R\}$, where r_l is the measured distance of an obstacle to the sensor rotating axis at direction ϕ_l). The scan measurements are acquired by the laser range finder with a given angular resolution $\Delta\phi = \phi_l - \phi_{l-1}$. Besides, the distance r_l is affected by a systematic error, ϵ_s, and a random error, ϵ_r , usually assumed to follow a Gaussian distribution with zero mean and variance σ_r^2. Previously to segment the scan data, the proposed system compensates this systematic error and the error due to the robot motion [8]. Finally, at the same time that these errors are corrected, rupture points can be detected. A rupture point is defined as a discontinuity during the laser measurement. Our laser sensor is a SICK Laser Measurement System LMS200, and this sensor returns a predefined binary data to indicate this occurrence.

III. Laser Scan Data Segmentation

Segmentation is a process whose aim is to classify each scan data into several groups, each one of them is associated to different surfaces of the environment. In our approach, the segmentation is achieved in two consecutive steps. Firstly, scan data is segmented using the adaptive breakpoint detector [4]. This algorithm permits to reject isolated range readings, but it provides an undersegmentation of the laser scan, i.e. extracted segments between breakpoints typically group two or more different structures (see Fig. 2a). In order to avoid this problem, a second segmentation criterion is applied into each segment. This one is based on the curvature associated to each range reading: consecutive range readings belong to the same segment while their curvature values are similar. To perform this segmentation task, the adaptive curvature function associated to each segment of the laser scan is obtained [8]. Fig. 2b shows the curvature function associated to the segment A in Fig. 2a. Curvature functions basically describe how much a curve bends at each point. Peaks of the curvature function correspond to the corners of the represented curve and their height depends on the angle at these corners. Flat segments whose average value is larger than zero are related to curve segments and those whose average value is equal to zero are related to straight line segments (see Fig. 2b).

IV. Landmark Extraction and Characterisation

As it can be appreciated in Fig. 2b, the adaptive curvature function can directly provide three different natural landmarks: line segments, corners and curve segments [8]. However, our experiments have shown us that the slope of these line segments

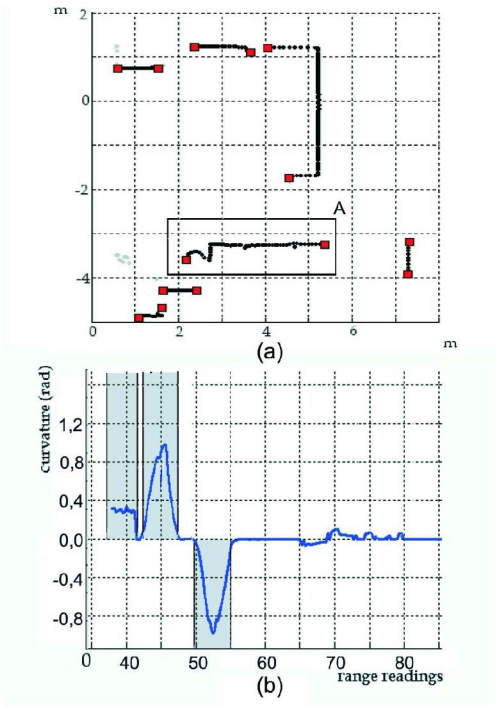

Fig. 2. Segment of a laser scan (□-breakpoints); and b) adaptive curvature function associated to segment A in a). Two line segments and one curve segments has been extracted

or the centre of curvature associated to these curve segments weakly depend on the position of the segments with respect to the robot. This problem can be avoided by fitting a model to the set of range readings that defines each line or curve segment. Thus, line and curve segments can be used as stable landmarks. Besides, real and virtual corners and edges are also extracted and characterised. In this section, the process to characterise each type of landmark is presented.

A. Line Segments

There are several approaches for line fitting. Thus, the parameters of a straight-line in slope-intercept form can be determined using the equations for linear regression [11]. Then, the resulting line can be converted into the normal form representation

$$xcos\theta + ysin\theta = d \tag{1}$$

being θ the angle between the x axis and the normal of the line and d the perpendicular distance of the line to the origin. Under the assumption of error free laser bearings, the covariance of the angle and distance estimate of the line can be derived. However, the problem of fitting a set of n points in Cartesian coordinates to a straight-line model using linear regression is based on the assumption that the uncertainty C_i associated with each y_i and x_i values are known exactly. In our case, the points being processed in Cartesian coordinates are the result of a nonlinear transformation of points from polar coordinates.

This makes errors in both Cartesian coordinates correlated [5], i.e. all terms of the covariance matrix, $C_{x,y}$, associated to a range reading i in Cartesian coordinates can be non-zero ones. Therefore, a better approach for line fitting is to minimize the sum of square perpendicular distances of range readings to lines. This yields a nonlinear regression problem which can be solved for polar coordinates [2]. The line in the laser range finder's polar coordinate system is represented as

$$rcos(\theta - \phi) = d \tag{2}$$

where θ and d are the line parameters (Eq. (1)). The orthogonal distance di of a range reading, $(r, \theta)_i$, to this line is

$$d_i = r_i cos(\theta - \phi_i) - d \tag{3}$$

and the sum of squared errors can be defined as

$$S_l(b) = \sum_{i=1}^{n} {d_i}^2 = \sum_{i=1}^{n} (r_i(\theta - \phi_i) - d)^2 \tag{4}$$

being n the number of range readings that belong to the line segment and $b = (\theta \;\; d)^T$ the parameter vector. Arras and Siegwart [2] propose to weight each single point by a different value w_i that depends on the variance modelling the uncertainty in radial and angular direction. In our case, uncertainties in range and bearing are the same for every range reading, so the weights for each point in polar coordinates are also equal. Therefore, we have not used these weights. The model parameters of the line (θ, d) can be obtained by solving the nonlinear equation system to minimize (4). The solution can be used in Cartesian form for computation reasons [2]:

$$\begin{aligned} \theta &= \tfrac{1}{2} \arctan\left(\frac{-2\sum_i (\bar{y}-y_i)(\bar{x}-x_i)}{\sum_i [(\bar{y}-y_i)^2 - (\bar{x}-x_i)^2]}\right) = \tfrac{1}{2} \arctan \tfrac{N}{D} \\ d &= \bar{x}\cos\theta + \bar{y}\sin\theta \end{aligned} \tag{5}$$

where $\bar{x} = \sum r_i \cos\phi_i / n$ and $\bar{y} = \sum r_i \sin\phi_i / n$.

In order to provide precise feature estimation, it is not only necessary to extract the feature parameter vector, but also to represent uncertainties and to propagate them from single range reading measurements to all stages involved in the feature estimation process. Assuming that the individual measurements are independent, the covariance matrix of the estimated line parameters (θ, d) can be calculated as [5]

$$C_{\theta,d} = \sum_i^n J_i C_{xyi} J_i^T \tag{6}$$

where the terms J_i represent the Jacobians for each point i and are obtained as follows

$$\begin{aligned} J_{1,1} &= \frac{\partial\theta}{\partial x_i} = \frac{(\bar{y}-y_i)D + (\bar{x}-x_i)N}{N^2+D^2} \\ J_{1,2} &= \frac{\partial\theta}{\partial y_i} = \frac{(\bar{x}-x_i)D + (\bar{y}-y_i)N}{N^2+D^2} \\ J_{2,1} &= \frac{\partial d}{\partial x_i} = \frac{1}{n}\cos\theta + (\bar{y}\cos\theta - \bar{x}\sin\theta)\frac{(\bar{y}-y_i)D + (\bar{x}-x_i)N}{N^2+D^2} \\ J_{2,2} &= \frac{\partial d}{\partial y_i} = \frac{1}{n}\sin\theta + (\bar{y}\cos\theta - \bar{x}\sin\theta)\frac{(\bar{x}-x_i)D + (\bar{y}-y_i)N}{N^2+D^2} \end{aligned} \tag{7}$$

being N and D the numerator and denominator of the expression of θ (5).

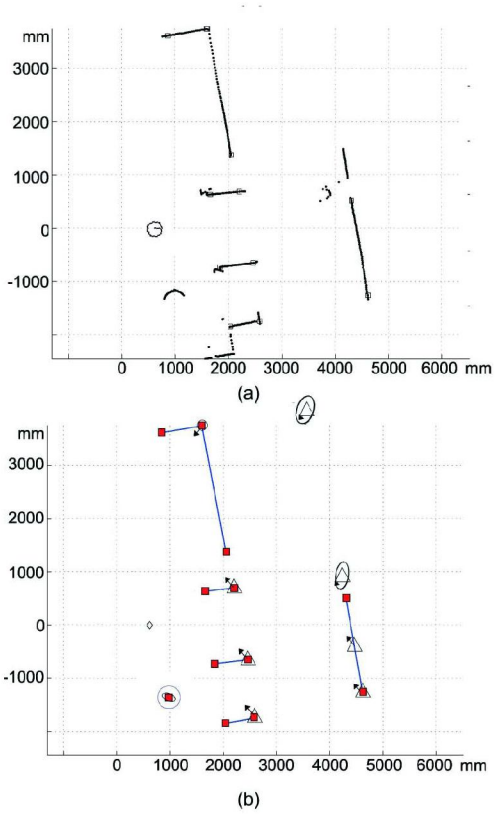

Fig. 3. 2D LASER SCAN; AND B) SEGMENTATION AND LANDMARK DETECTION ASSOCIATED TO A). (□ -LINE SEGMENTS END-POINTS, o -REAL CORNERS, △ -VIRTUAL CORNERS, → -CORNER ORIENTATIONS). CIRCLES ARE ALSO REPRESENTED.

Fig. 3b shows the line segments extracted using the described approach and corresponding to the laser scan in Fig. 3a. The end-points of each line segment are determined by the intersection between this line and the two lines which are perpendiculars to it and pass through the first and last range readings.

B. Curve Segments

A curve segment of constant curvature can be considered as an arc of a circle which is basically described by its center of curvature (x_c, y_c) and its radius ρ. Circle fitting problem estimates these parameters finding the vector $b = (x_c, y_c, \rho)$ that minimizes

$$S_c(b) = \sum_{i=1}^{n} [(x_i - x_c)^2 + (y_i - y_c)^2 - \rho^2]^2 \tag{8}$$

where $\{(x, y)\}_{i=1...n}$ is the set of range readings that defines the curve segment in Cartesian coordinates. However, the covariance matrix associated to each range reading in Cartesian coordinates is different and then, each term in Eq. (8) must be weighted by a value which will take into account the measurement uncertainty. In our particular case, this can be avoided if we work in polar coordinates, because in this coordinate system, the covariance matrix is the same for each

reading. Therefore, our aim is to find the circle $(x_i - x_c)^2 + (y_i - y_c)^2 - \rho^2 = 0$ where $x = r\cos\phi$, $y = r\sin\phi$, $x_c = r_c\cos\phi_c$ and $y_c = r_c\sin\phi_c$, yielding

$$r^2 + r_c^2 - 2rr_c\cos(\phi - \phi_c) - \rho^2 = 0 \tag{9}$$

To minimize $S_c(b) = S_c(r_c, \phi_c, \rho)$, finding the parameter vector b, we use the Levenberg-Marquardt algorithm [7]. This algorithm approximates S_c as a linear function of b, $\hat{S}_c$:

$$S_c(b) \approx \hat{S}_c(b) = \sum(d_i(b_k) + \nabla d_i(b_k)\cdot b)^2 \tag{10}$$

where $d_i(b) = r_i^2 + r_c^2 - 2r_i r_c\cos(\phi_i - \phi_c) - \rho^2$ and $\nabla d_i(b)$ is the gradient of $d_i(b)$. This estimation is valid within a certain trust region radius. The algorithm begins using an initial parameter vector b_0. Then, the derivation considers how to minimize $\hat{S}_c(p)$. A whole description about this method is described in [7]. To obtain this parameter vector $b_0 = (x_c, y_c, \rho)$, we use the equation of a circle passing through three given points, (x_1, y_1), (x_2, y_2) and (x_3, y_3):

$$\begin{array}{l} y_c = (a\cdot f - c\cdot d)/(b\cdot d - a\cdot e) \\ x_c = (y_c\cdot b)/a + c/a \\ \rho = \sqrt{((x_1 - x_c)^2 + (y_1 - y_c)^2)} \end{array} \tag{11}$$

where a, b, c, d, e and f are given by

$$\begin{array}{ll} a = 2(x_2 - x_1) & b = 2(y_2 - y_1) \\ c = x_1^2 + y_1^2 - x_2^2 - y_2^2 & d = 2(x_3 - x_1) \\ e = 2(y_3 - y_1) & f = x_1^2 + y_1^2 - x_3^2 - y_3^2 \end{array} \tag{12}$$

From these expressions (see Appendix), an estimation of the curve segment uncertainty, represented as $C(r_c, \theta_c, \rho)$, can be derived. Fig. 3a presents a real laser scan containing columns and tree-like elements that are extracted and represented (center and circumference) in Fig. 3b. Uncertainties associated to the center of the circles are also shown.

C. Real Corners

Corners are due to change of surface being scanned or to change in the orientation of the scanned surface. Thus, they are not associated to laser scan discontinuities. In order to obtain the corner location, it must be taken into account that failing to identify the correct corner point in the data can lead to large errors especially when corner is distant from the robot. Therefore, it is not usually a good option to locate the corner in one of the scan range readings. Other option is to extract the corner taking into account the two lines associated to it. Thus, corner can be detected as the furthest point from a line defined by the two non-touching end-points of the lines or by finding that point in the neighborhood of the initial corner point, which gives the minimum sum of error variances of both lines [5]. In our case, the existence of a corner can be determined from the curvature function [8], but its characterization (estimation of the mean pose and uncertainty measurement) is conducted using the two lines which generate the corner. Therefore a corner will be always defined as the intersection of two lines. Once a corner is detected, its position (xc,yc) is estimated as the intersection of the two lines which generate it. If these lines are characterized by (θ_1, d_1) and (θ_2, d_2), the corner point (x_c, y_c) will be the intersection of these lines, i.e.

$$\begin{array}{l} x_c\cos\theta_1 + y_c\sin\theta_1 - d_1 = 0 \\ x_c\cos\theta_2 + y_c\sin\theta_2 - d_2 = 0 \end{array} \tag{13}$$

Resolving (13), we obtain a value for (x_c, y_c):

$$x_c = \frac{d_1\sin\theta_2 - d_2\sin\theta_1}{\sin(\theta_2 - \theta_1)} \quad y_c = \frac{d_2\cos\theta_1 - d_1\cos\theta_2}{\sin(\theta_2 - \theta_1)} \tag{14}$$

The corner orientation α_c can be also calculated as the bisector of the angle defined by these two lines. Finally, the covariance of the estimated corner parameters can be calculated depending on the noise in the line parameters (see Appendix). Fig. 3b illustrates the real corner detection results. Corner poses and uncertainties have been marked.

D. Virtual Corners

As it is pointed out by Madhavan and Durrant-Whyte [6], one of the main problems of a localization algorithm which is only based on corner detection is that the set of detected natural landmarks at each time step can be very reduced. This generates a small observation vector that does not provide a good estimation of the robot's pose. To attenuate this problem, we include in this work a new natural landmark which can be used in the same way that real corners: the virtual corner. Virtual corners are defined as the intersection of extended line segments which are not previously defined as real corners. The virtual corner described in this paper is related to the virtual edge anchor [10]. However, in our case, the virtual corner is related to the line segments previously extracted. The virtual edge anchor is found without explicit line extraction and offers higher robustness against partial occlusion and noise effects. In our approach, the robust detection of lines is directly related to the adaptive curvature estimation algorithm and the process used for line characterization.

Finally, virtual corners can be characterized using the same process described for a real corner in Section IV-C. Fig. 3b shows virtual corners (poses and uncertainties) associated to laser scan in Fig. 3a. The error propagation due to the distances from the lines to the virtual corners can be appreciated in their uncertainty ellipses. Fig. 3b also presents that virtual corners increases the size of the extracted observation vector.

E. Edges

The adaptive breakpoint detector searches for large discontinuity values in the laser scan data. Range readings that define this discontinuity are marked as breakpoints. Edges are defined as breakpoints associated to end-points of plane surfaces [12]. To satisfy this condition, the portion of the environment where the breakpoint is located must be a line segment and it must

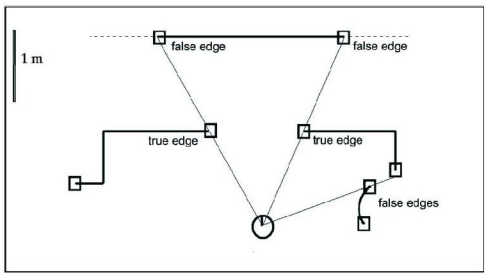

Fig. 4. AN EDGE IS DEFINED AS A BREAKPOINT ASSOCIATED TO THE END-POINT OF A PLANE SURFACE WHICH IS NOT OCCLUDED OBSTACLES.

not be occluded by any other obstacle. This condition is true if the breakpoint is nearer to the robot than the other breakpoint defined by the same large discontinuity (see Fig. 4). Edges are characterised by the Cartesian position (x, y) of the breakpoint and by the orientation of the plane surface described by the line segment, α. Thus, the covariance of the estimated edge parameters (x_e, y_e, α_e) can be approximated as

$$C_{x_e y_e \alpha_e} = \begin{bmatrix} \sigma_x^2 & \sigma_{xy} & 0 \\ \sigma_{xy} & \sigma_y^2 & 0 \\ 0 & 0 & \sigma_\alpha^2 \end{bmatrix} \quad (15)$$

where σ_α^2 is the orientation variance associated to the line segment.

V. EXPERIMENTAL RESULTS

The feature extraction system has been implemented on an ActivMedia Pioneer2-AT equipped with a LMS200 sensor. Algorithms have been programmed in C++ on a 855 MHz PC. The experiments presented in this section are taken from two different indoor settings, a laboratory (Fig. 5a) and a corridor (Fig. 5b). Experiments has been focussing in order to obtain an evaluation of the proposed method about the speed (t), robustness ($r_{landmark}$, % of times a feature has been detected divided by the % of times it has been visible), the total number of detected landmarks (k) and the number of multiple detections of the same feature (k_m). Table I shows the average values for these experiments composed of 50 scans.

TABLE I.
EXPERIMENTAL RESULTS OF THE ALGORITHMS

	t[ms]	r_{rc}	r_{vc}	r_{ls}	r_{cs}	r_e	k	k_m
Test 1	25	0,91	0,98	0,98	0,87	0,94	21	0,02
Test 2	22	0,94	0,97	0,98	0,84	0,96	10	0,09

where r_{rc}, r_{vc}, r_{ls}, r_{cs} and r_e represent the robustness of the real corners, virtual corners, line segments, circle segments and edges extraction, respectively. The laboratory is for obvious reasons more furnished than the corridor and hence contains more natural landmarks. Experiments show that usually there are not duplicate landmarks. Moreover circle segments are, generally, less robust than other extracted features. Finally, it must be noted that the total time necessary to process the scan data is very reduced. It allows a future real time localisation.

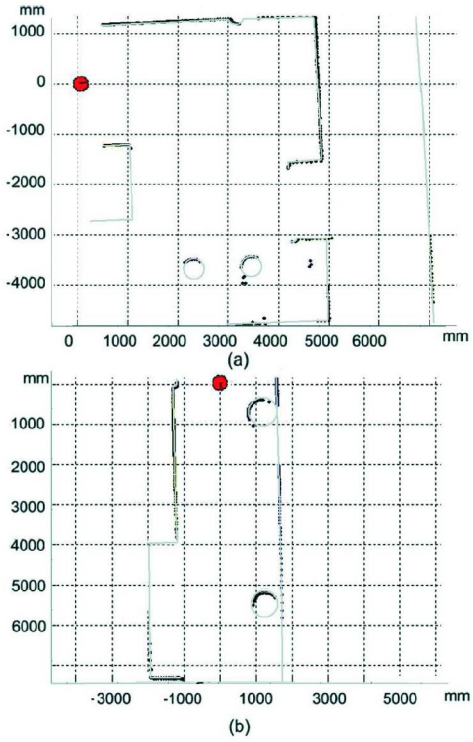

Fig. 5. SCANS OF TWO INDOOR ENVIRONMENT TO TEST THE PROPOSED SYSTEM. REAL LAYOUTS ARE SUPERIMPOSED IN THE IMAGES.

VI. CONCLUSION AND FUTURE WORKS

In this paper an algorithm for feature extraction and characterisation from laser scan data is presented. This algorithm segments the laser scan using an adaptive noise removal. This permits to detect features at a wide range of scales for a fixed set of detection parameters. This feature are characterized not only by their parameter vectors, but statistical information is also obtained. Then, the algorithm can provide a large set of landmarks to the later mapping and localisation modules thus reducing the time required for a mobile robot to successfully localise itself. The accuracy and robustness of the proposed method was demonstrated in a real indoor environment satisfying real time requirements. Future works will focus in comparing our system with other different methods and use these extracted landmarks in a whole SLAM process.

ACKNOWLEDGMENT

This work has been partially granted by the Spanish Ministerio de Educacion y Ciencia (MEC) and FEDER funds Project no. TIN2005-01359.

REFERENCES

[1] M. Altermatt, A. Martinelli, N. Tomatis and R. Siegwart, SLAM with Corner Features Based on a Relative Map, IEEE/RSJ International Conference on Intelligence Robots and Systems, pp. 1053-1058, 2004.

[2] K.O. Arras and R. Siegwart, "Feature extraction and scene interpretation for map based navigation and map building", in: Proceedings of SPIE, Mobile Robotics XII, volume 3210, 1997.

[3] A. Bandera, J.M. Perez-Lorenzo, J.P. Bandera and F. Sandoval, "Mean shift based clustering of Hough domain for fast line segment detection", Pattern Recognition Letters 27(6) (2006) 578-586.
[4] G. A. Borges and M. Aldon, "Line extraction in 2D range images for mobile robotics", Journal of Intelligent and Robotic Systems 40, pp. 267-297, 2004.
[5] A. Diosi and L. Kleeman, "Uncertainty of line segments extracted from static sick pls laser scans", Technical Report MECSE-26-2003, Department of Electrical and Computer Systems Engineering, Monash University, 2003.
[6] R. Madhavan and H.F. Durrant-Whyte, "Natural landmark-based autonomous vehicle navigation", Robotic and Autonomous Systems 46, pp. 79-95, 2004.
[7] J.C. Nash, "Compact numerical methods for computers: linear algebra and function minimisation", Adam Hilger Ltd., 1979.
[8] P. Núñez, R. Vázquez-Martín, J.C. del Toro, A. Bandera, and F. Sandoval, "Feature extraction from laser scan data based on curvature estimation for mobile robotics", in: Proc. of the IEEE Int. Conf. on Robotics and Automation, 2006, pp. 1167-1172.
[9] J. D. Tardós, J. Neira, P. M. Newman and J. J. Leonard, .Robust mapping and localization in indoor environments using sonar data., Int. Journal of Robotics Research, pp. 311-330, 2002.
[10] J.Weber, L. Franken, K. Jörg and E. Puttkamer, "Reference scan matching for global self-localization", Robotics and Automation 40 (2002) 99-110.
[11] L. Zhang and B.K. Ghosh, "Line segment based map building and localization using 2D laser rangefinder", in: "Proc. of the IEEE Int. Conf. on Robotics and Automation", 2000, pp. 2538-2543.
[12] S. Zhang, L. Xie, M.D. Adams and F. Tang, "Geometrical Feature Extraction Using 2D Range Scanner", Int. Conf. on Control and Automation, pp. 901-905, 2003.

APPENDIX

I. DERIVING THE COVARIANCE MATRIX ASSOCIATED TO A CIRCLE SEGMENT

A circle is characterised using its center and radius, (x_c, y_c, ρ). To calculate the uncertainty associated to a circle segment, $C_{x_c,y_c,\rho}$, we define $\mathbf{b}$ as $[x_c \;\; y_c \;\; \rho]^T = f(x_c, y_c, \rho)$. Then the first order Taylor expansion of $\mathbf{b}$ is

$$\Delta b = \nabla f(\mathbf{x},\mathbf{y})\Delta[\mathbf{x}^T \;\; \mathbf{y}^T]^T = J\Delta[\mathbf{x}^T \;\; \mathbf{y}^T]^T \tag{16}$$

being J the Jacobian of $f(\mathbf{x},\mathbf{y})$, whose elements are obtained taking int account Eqs. (11) and (12). If we would calculate this Jacobian, we can approximate the covariance as

$$C_{(x_c,y_c,\rho)} = JC_{x_1y_1x_2y_2x_3y_3}J^T \tag{17}$$

To obtain an approximate covariance and calculate the Jacobian, we can consider

$$y_c = \frac{af-cd}{bd-ae} = \frac{N}{D} \quad R = \rho^2 \tag{18}$$

where the constants a, b, c, d, e, and f are defined in (12). Then, the elements of the Jacobian can be calculated as

$$J_{1,1} = \frac{\partial x_c}{\partial x_1} = \frac{\partial y_c}{\partial x_1}\cdot\frac{b}{a} + \frac{2}{a^2}\cdot(by_c + x_1a + c) \tag{19}$$

$$J_{1,2} = \frac{\partial x_c}{\partial y_1} = \frac{\frac{\partial y_c}{\partial y_1}\cdot b + 2(y_1 - y_c)}{a} \tag{20}$$

$$J_{1,3} = \frac{\partial x_c}{\partial x_2} = \frac{\partial y_c}{\partial x_2}\cdot\frac{b}{a} - \frac{2}{a^2}\cdot(by_c + x_2a + c) \tag{21}$$

$$J_{1,4} = \frac{\partial x_c}{\partial y_2} = \frac{\frac{\partial y_c}{\partial y_2}\cdot b + 2(y_c - y_2)}{a} \tag{22}$$

$$J_{1,5} = \frac{\partial x_c}{\partial x_3} = \frac{\partial y_c}{\partial x_3}\cdot\frac{b}{a} \quad J_{1,6} = \frac{\partial x_c}{\partial y_3} = \frac{\frac{\partial y_c}{\partial y_3}\cdot b}{a} \tag{23}$$

$$J_{2,1} = \frac{\partial y_c}{\partial x_1} = \frac{2(x_1\cdot(a-d)+c\cdot f)\cdot D - 2(e-b)\cdot N}{D^2} \tag{24}$$

$$J_{2,2} = \frac{\partial y_c}{\partial y_1} = \frac{2y_1(a-d)\cdot D - 2(1-d)N}{D^2} \tag{25}$$

$$J_{2,3} = \frac{\partial y_c}{\partial x_2} = \frac{2x_2\cdot(f+d)\cdot D + 2eN}{D^2} \tag{26}$$

$$J_{2,4} = \frac{\partial y_c}{\partial y_2} = \frac{2y_2dD - 2dN}{D^2} \tag{27}$$

$$J_{2,5} = \frac{\partial y_c}{\partial x_3} = \frac{-2(ax_2 - c)\cdot D - 2bN}{D^2} \tag{28}$$

$$J_{2,6} = \frac{\partial y_c}{\partial y_3} = \frac{-2y_3aD + 2aN}{D^2} \tag{29}$$

$$J_{3,1} = \frac{\partial \rho}{\partial x_1} = R^{-1/2}(A(1 - \frac{\partial x_c}{\partial x_1}) - B\frac{\partial y_c}{\partial x_1}) \tag{30}$$

$$J_{3,2} = \frac{\partial \rho}{\partial y_1} = R^{-1/2}(B(1 - \frac{\partial y_c}{\partial y_1}) - A\frac{\partial x_c}{\partial y_1}) \tag{31}$$

$$J_{3,3} = \frac{\partial \rho}{\partial x_2} = -R^{-1/2}(A\frac{\partial x_c}{\partial x_2} - B\frac{\partial y_c}{\partial x_2}) \tag{32}$$

$$J_{3,4} = \frac{\partial \rho}{\partial y_2} = -R^{-1/2}(B\frac{\partial y_c}{\partial y_2} + A\frac{\partial x_c}{\partial y_2}) \tag{33}$$

$$J_{3,5} = \frac{\partial \rho}{\partial x_3} = -R^{-1/2}(A\frac{\partial x_c}{\partial x_3} + B\frac{\partial y_c}{\partial x_3}) \tag{34}$$

$$J_{3,6} = \frac{\partial \rho}{\partial y_3} = -R^{-1/2}(B\frac{\partial y_c}{\partial y_3} + A\frac{\partial x_c}{\partial y_3}) \tag{35}$$

being $A = x_1 - x_c$ and $B = y1 - yc$.

II. DERIVING THE COVARIANCE MATRIX ASSOCIATED TO A CORNER

After the first order Taylor expansion, the covariance associated to a corner, represented as $C_{x_cy_c\alpha_c}$, can be aproximated as

$$C_{x_cy_c\alpha_c} = JC_{r_1\alpha_1r_2\alpha_2}J^T \tag{36}$$

being $C_{r_1\alpha_1r_2\alpha_2}$ the covariance matrix associated to the lines which generate the corner. Taking into account that $\alpha = (\alpha_1 - \alpha_2)/2$, the elements of the Jacobian J can be calculated as follows

$$J_{1,1} = \frac{\partial x_c}{\partial r_1} = \frac{\sin\alpha_2}{\sin(\alpha_2 - \alpha_1)} \tag{37}$$

$$J_{2,1} = \frac{\partial x_c}{\partial \alpha_1} = \frac{-r_2\cos\alpha_1\sin(\alpha_2 - \alpha_1) + A\cos(\alpha_2 - \alpha_1)}{\sin^2(\alpha_2 - \alpha_1)} \tag{38}$$

$$J_{3,1} = \frac{\partial x_c}{\partial r_2} = \frac{-\sin\alpha_1}{\sin(\alpha_2 - \alpha_1)} \tag{39}$$

$$J_{4,1} = \frac{\partial x_c}{\partial \alpha_2} = \frac{r_1\cos\alpha_2\sin(\alpha_2 - \alpha_1) - A\cos(\alpha_2 - \alpha_1)}{\sin^2(\alpha_2 - \alpha_1)} \tag{40}$$

$$J_{1,2} = \frac{\partial y_c}{\partial r_1} = \frac{-\cos\alpha_2}{\sin(\alpha_2 - \alpha_1)} \tag{41}$$

$$J_{2,2} = \frac{\partial y_c}{\partial \alpha_1} = \frac{-r_2\sin\alpha_1\sin(\alpha_2 - \alpha_1) + B\cos(\alpha_2 - \alpha_1)}{\sin^2(\alpha_2 - \alpha_1)} \tag{42}$$

$$J_{3,2} = \frac{\partial y_c}{\partial r_2} = \frac{\cos\alpha_1}{\sin(\alpha_2 - \alpha_1)} \tag{43}$$

$$J_{4,2} = \frac{\partial y_c}{\partial \alpha_2} = \frac{r_1\sin\alpha_2\sin(\alpha_2 - \alpha_1) - B\cos(\alpha_2 - \alpha_1)}{\sin^2(\alpha_2 - \alpha_1)} \tag{44}$$

$$J_{1,3} = \frac{\partial \alpha_c}{\partial r_1} = 0 \quad J_{2,3} = \frac{\partial \alpha_c}{\partial \alpha_1} = \frac{1}{2} \tag{45}$$

$$J_{3,3} = \frac{\partial \alpha_c}{\partial r_2} = 0 \quad J_{4,3} = \frac{\partial \alpha_c}{\partial \alpha_2} = -\frac{1}{2} \tag{46}$$

where $A = r_1\sin\alpha_2 - r_2\sin\alpha_1$ and $B = r_2\cos\alpha_1 - r_1\cos\alpha_2$.